

Article ID:

Disbond detection with piezoelectric wafer active sensors in RC structures strengthened with FRP composite overlays

Victor Giurgiutiu^{1†}, Kent Harries^{2‡}, Michael Petrou^{2†}, Joel Bost^{1§}, Josh B. Quattlebaum^{2*}

1. Department of Mechanical Engineering, University of South Carolina, USA

2. Department of Civil and Environmental Engineering, University of South Carolina, USA

Abstract: The capability of embedded piezoelectric wafer active sensors (PWAS) to perform in-situ nondestructive evaluation (NDE) for structural health monitoring (SHM) of reinforced concrete (RC) structures strengthened with fiber reinforced polymer (FRP) composite overlays is explored. First, the disbond detection method were developed on coupon specimens consisting of concrete blocks covered with an FRP composite layer. It was found that the presence of a disbond crack drastically changes the electromechanical (E/M) impedance spectrum measured at the PWAS terminals. The spectral changes depend on the distance between the PWAS and the crack tip. Second, large scale experiments were conducted on a RC beam strengthened with carbon fiber reinforced polymer (CFRP) composite overlay. The beam was subject to an accelerated fatigue load regime in a three-point bending configuration up to a total of 807,415 cycles. During these fatigue tests, the CFRP overlay experienced disbonding beginning at about 500,000 cycles. The PWAS were able to detect the disbonding before disbond damage was observed. These preliminary results demonstrate the potential of PWAS technology for SHM of RC structures strengthened with FRP composite overlays.

Keywords: FRP composite overlays; composite strengthening and rehabilitation; structural health monitoring; piezoelectric wafer active sensors; E/M impedance; aging infrastructure; disbond damage; PWAS

1 Introduction

1.1 Composite overlays

Composite overlays are thin sheets of fiber reinforced polymeric material adhesively bonded to conventional construction engineering materials. Candidate polymeric systems include epoxy, polyester, and vinylester. Fibers can be E-glass, carbon, aramid or hybrids thereof. Fiber systems come in a variety of forms including unimpregnated woven or non-woven fabrics, preimpregnated sheets (prepregs) and precured laminates. An FRP system may be applied in a wet lay-up procedure (fabrics), a dry lay-up procedure including a curing phase (prepregs), or as an adhesive application (precured laminates). In wet lay-up and prepreg application the adhesive bonding the FRP to the substrate is the polymeric resin itself. For precured rigid sheets or strips, a separate adhesive

material needs to be used. Structural upgrades, including seismic rehabilitation, with composite overlays offer considerable advantages in terms of weight, volume, labor cost, specific strength and stiffness, over other retrofit strategies. However, one critical issue raised by structural engineers is the still unknown in-service durability of these new material systems. Their ability to safely perform after prolonged exposure to service loads and environmental factors must be ascertained before wide acceptance in the construction engineering community is achieved.

1.2 Strength and durability of composite overlaid structures

The degradation and loss of performance of composite overlays on concrete or masonry substrate may result from: (a) degradation of the composite overlay; (b) deterioration of the concrete substrate; and (c) loss of adhesion between the overlay and the substrate. The degradation of composite materials and the fatigue of concrete structures have been extensively researched elsewhere (Williams, 1984; Mallick, 1993; ACI 1987; Shah *et al.*, 1995). However, the durability of the bond between the composite and the substrate remains a critical issue. A sudden loss of bond through wide area delamination can lead to a catastrophic failure of the structure. Hence, the loss of adhesion between

Correspondence to: Victor Giurgiutiu, Dept. of Mechanical Engineering, University of South Carolina, 300 North Street, Columbia SC 29208

Tel: 803-777-8018; **Fax:** 803-777-0106

E-mail: victorg@sc.edu

[†]Associate Professor; [‡]Assistant Professor; [§]Undergraduate Research Assistant; ^{*}Graduate Research Assistant

Received date: 2003-11-11; **Accepted date:** 2003-11-16

the composite overlay and the substrate remains a critical factor. Maintenance of good adhesion between the composite overlay and the substrate structure is of paramount importance for assuring long-term performance and for preventing failure of such structural upgrades and repairs. To date, this phenomenon has not been extensively studied and is insufficiently documented. The loss of adhesion and performance degradation can be traced to the interface between the composite overlay and the concrete substrate. The bond degradation manifests itself in the form of disbonding cracks and delaminations. If the disbonding becomes widespread, significant loss of load-transfer capabilities can occur. Crack propagation is promoted by combined hygro-thermal-mechanical cycling. Crack propagation can be delayed and even prevented by increasing the inherent fracture toughness at the composite/substrate interface.

The use of fiber reinforced polymer (FRP) composite materials for structural repair and seismic strengthening applications has been studied extensively in the last decade and is now seeing its way into regular commercial applications. Numerous experimental and analytical studies have demonstrated the ability of externally bonded FRP materials to improve the performance of reinforced concrete structural members. Improvement may take the form of enhanced load carrying capacity, stiffness or ductility, improved performance under cyclic or repeated loading or enhanced environmental durability. Any improvement realized by an externally bonded repair system, however, is limited by the performance of the bond of the repair material to the substrate.

Failure of FRP-strengthened reinforced concrete beams may take a variety of forms including all of those associated with conventional concrete beams (Buyukozturk and Hearing, 1998). Most all studies of FRP-strengthened concrete beams, however, report some form of FRP bond failure (Quattlebaum, 2003). Failures that are specifically due to bond failure can be characterized by the type of delamination and where the delamination initiates. Two types of delamination have been reported; cover delamination and FRP delamination. Cover delamination is a failure of the concrete in the plane of the steel reinforcement while FRP delamination is a failure in the plane along the FRP/concrete interface.

As described by Triantafillou *et al.* (2001) and Sebastian (2001), disbonding of FRP from the soffit of a concrete beam may be initiated either:

a. At a stress raiser along the length of the FRP (typically an internal flexure or shear crack in the concrete) and propagate away from this location toward the FRP termination; or,

b. At the termination of the FRP material and propagate toward the midspan.

In either case, as the cracks propagate, the FRP disbonds from the concrete substrate. It is important to note that such disbonding cracks typically propagate through

the concrete substrate rather than through the FRP or adhesive.

1.3 Piezoelectric wafer active sensors and the electromechanical impedance technique

Piezoelectric wafer active sensors (PWAS) are inexpensive and minimally invasive devices that are permanently mounted to structures in order to excite and detect elastic waves. PWAS can be used in conjunction with either propagating wave methods such as pitch-catch and pulse-echo, or with standing wave methods such as the high-frequency electromechanical (E/M) impedance technique. The E/M impedance technique is able to measure directly the high-frequency local impedance of the structure in the form of the real part of the electromechanical impedance of the PWAS that is attached to the structure (Giurgiutiu and Zagari, 2001). This property originates in the piezoelectric coupling inherent in the PWAS material that couples the mechanical strain, S_{ij} , and stress, T_{kl} , to the electrical field, E_k , and electrical displacement, D_j , in the form:

$$\begin{aligned} S_{ij} &= s_{ijkl}^E T_{kl} + d_{kij} E_k \\ D_j &= d_{jkl} T_{kl} + \varepsilon_{jk}^T E_k \end{aligned} \quad (1)$$

where s_{ijkl}^E is the mechanical compliance of the material measured at zero electric field ($E = 0$), ε_{jk}^T is the dielectric permittivity measured at zero mechanical stress ($T = 0$), and d_{kij} represents the piezoelectric coupling coefficient. Figure. 1 shows schematically how the PWAS transducer couples the electrical voltage and current with the structural dynamics represented by the equivalent frequency-dependent mass, $m_e(\omega)$, stiffness, $k_e(\omega)$, and damping, $c_e(\omega)$. Denoting the structural impedance by

$$Z_{\text{str}}(\omega) = [k_e(\omega) - \omega^2 m_e(\omega) + i\omega c_e(\omega)] / i\omega \quad (2)$$

and the PWAS impedance by $Z_{\text{PWAS}}(\omega)$, one can write the electromechanical impedance $Z(\omega)$ as measured at the PWAS terminals as

$$Z(\omega) = \left[i\omega C \left(1 - \kappa_{31}^2 \frac{Z_{\text{str}}(\omega)}{Z_{\text{PWAS}}(\omega) + Z_{\text{str}}(\omega)} \right) \right]^{-1} \quad (3)$$

where C is the zero-load capacitance of the PWAS transducer, and κ_{31} is the electro-mechanical cross coupling coefficient of the PWAS transducer, $\kappa_{31} = d_{31} / \sqrt{s_{11}^E \varepsilon_{33}^T}$. When mounted on a structural surface the PWAS couples its in-plane motion, excited by the applied oscillatory voltage through the piezoelectric effect, with the elastic-wave motion on the material surface. PWAS probes can act as both exciters and sensors of the elastic Lamb waves traveling in the material. If excited with a sustained harmonic signal of

certain frequencies, the PWAS induces a standing wave pattern in the support structure corresponding to the structural resonances. At high frequencies, the structural resonances are localized and highly sensitive to local damage. In contrast, low frequency resonances have a global nature, and are less sensitive to local damage and more sensitive to global boundary conditions. Because the E/M impedance method operates at very high frequencies, it is impervious to vibration and noise that appears during normal structural operation. The electro-mechanical impedance method is applied by scanning a predetermined frequency range in the hundreds of kHz frequency band and recording the complex impedance spectrum. By comparing the impedance spectra taken at various times during the service life of a structure, meaningful information can be extracted pertinent to structural degradation and the appearance of incipient damage. It must be noted that the frequency range must be high enough for the signal wavelength to be compatible with the defect size.

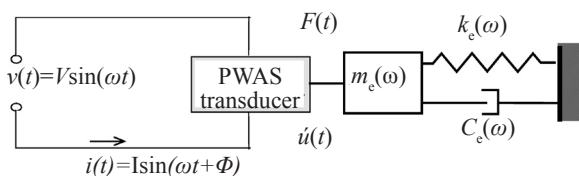


Fig. 1 Electro-mechanical coupling between the PZT transducer and the structure used in the E/M impedance method for structural health monitoring

The use of PWAS for high-frequency local modal sensing with the E/M impedance method has been pursued for various applications by Liang *et al.* (1994), Sun *et al.* (1994), Cudney and Inman (1998), Park *et al.* (2000), Pohl *et al.* (2001), Bois and Hochard (2002), Giurgiutiu *et al.* (1997, 1999, 2002), Zagari and Giurgiutiu (2001), and others. Applications of the E/M impedance method to the SHM of civil engineering structures were done by Ayres *et al.* (1996), Soh *et al.*

(2000), Saffi and Sayyah (2001), and Tseng *et al.* (2002, 2003). Recently, Bhalla and Soh (2003) studied the detection of earthquake induced damage in RC structure using the E/M impedance technique, while Koh and Chiu (2003) performed a finite-element simulation of the disbond detection of a composite repair patch using low frequency E/M impedance and transfer function methods.

The present paper presents experimental verification of the capability of PWAS to detect the disbonding of FRP composite overlays on reinforced concrete structures. Two types of experiments are presented, coupon tests and large-scale tests. The coupon tests were used to develop the disbond detection methodology based on changes in the E/M impedance spectrum in correlation with disbond cracks of various sizes. The large scale experiments used the E/M impedance method to monitor the disbond cracks induced during the fatigue testing of a 4.572-m long RC beam strengthened on its soffit with a 51-mm wide carbon fiber (CFRP) composite strip. Good correlation between the PWAS readings and the position and extent of disbond damage was observed. These preliminary results demonstrate the potential of PWAS technology for the structural health monitoring of RC structures strengthened with FRP composite overlays.

2 Coupon tests

Coupon tests were conducted to develop the disbond detection methodology based on changes in the E/M impedance spectrum in correlation with disbond cracks of various sizes.

2.1 Coupon tests specimens

Figure 2 shows the coupon specimen used during these tests. The specimens consisted of a concrete substrate having an FRP composite overlay applied on its upper surface. The concrete substrate was a 51mm \times 51mm \times 178mm concrete block fabricated in our laboratory. The FRP composite overlay consisted of glass fiber reinforced polyester (GFRP) fabricated in the

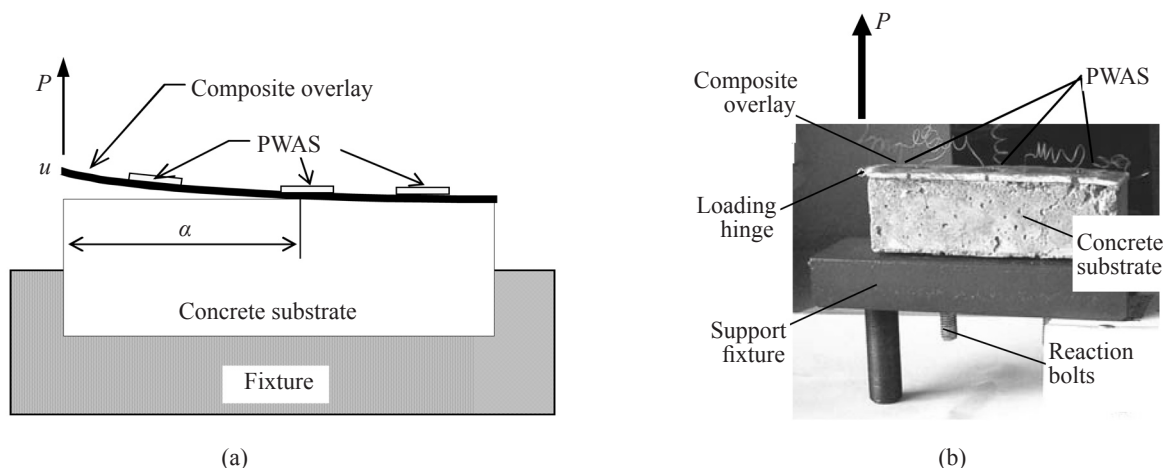


Fig. 2 Coupon test specimen for E/M impedance technique disbond detection: (a) specimen schematic; (b) actual specimen with the PWAS disbond sensors placed at 35-mm, 90-mm, and 145-mm from the loading hinge

laboratory from commercially available components. The composite overlay was 3.2 cm thick and 5 cm wide. During the block casting process, two anchor bolts (12.5 mm diameter) were inserted and set in place. These bolts attached the specimen to the test fixture and took up the reaction forces. During composite overlay fabrication, a loading hinge lead was inserted into the left end of the composite overlay (Fig. 2(b)). Three PWAS were applied to the top of the composite overlay at distances of 35 mm, 90 mm, and 145 mm from the loading hinge.

2.2 Coupon tests procedure

The testing consisted of applying a vertical force through the loading hinge at the tip of the composite overlay and increasing it under displacement control until a crack started to propagate. The loading was performed in displacement control; hence, the start of crack propagation was accompanied by a sharp decrease in the applied force. Subsequently, the displacement was kept constant until the crack propagation process was exhausted and the crack was arrested. At this point, the crack length was recorded, measurements were taken, and the loading was resumed. With this method, we were able to grow disbond cracks of increasing lengths between the composite overlay and the concrete substrate. In total, seven cracks of increasing length were propagated (cracks #0 through #6 in Fig. 3). More details about the fabrication and loading of these specimens can be found in Giurgiutiu *et al.* (2001).

2.3 E/M impedance spectroscopy for the coupon tests

Readings of the high frequency E/M impedance of each of the three PWAS were recorded and stored for each crack length. The frequency range used during these recordings was 100-600 kHz. During data post-processing, plots of the real part of the E/M impedance were assembled. As shown by Giurgiutiu and Zagari (2001), the real part of E/M impedance, $\text{Re}(Z)$, measured at the PWAS terminal reflects with fidelity the mechanical impedance of the structure at the PWAS location. As a crack propagates under the composite overlay, the underlying support conditions change. This change in support conditions induces a change in the resonance spectrum. Figure 3 shows how the plots of the E/M impedance spectrum of the three PWAS modify as the crack progresses. The PWAS #1, which is closest to the loading end, experiences these changes first. As seen in Fig. 3, the pristine spectrum of PWAS #1 has two well-damped peaks, one at around 200 kHz, the other at around 390 kHz. The damping of these peaks is provided by the concrete substrate through the bonding layer. As the tip of the disbonding crack #0 reaches almost to PWAS #1, the E/M impedance changes dramatically, with the two

resonance peaks amplitudes increasing very strongly and also shifting to lower frequencies. The increases in the peaks amplitudes are associated with a decrease in the damping effect of the concrete substrate, which is no longer bonded to the composite in the vicinity of PWAS #1. The downward frequency shift is associated with the reduction in the local support stiffness provided by the concrete to the composite overlay. As the disbond progresses, the composite overlay tends to vibrate as a locally free plate. Because the E/M impedance test is conducted at very high frequencies, the vibration modes are highly localized, and hence very sensitive to changes in the local boundary conditions. As the cracking progressed past PWAS #1, the change in the E/M impedance spectrum becomes even stronger. This situation corresponds to crack #1 in the PWAS #1 plot of Fig. 3. However, once the crack tip has passed the location of the PWAS #1, no more significant changes are observed in the E/M impedance spectrum. Thus, the spectra of PWAS #1 for cracks #2 through #5 are almost identical. (No recording exists for crack #6 on PWAS #1 because the sensor was damaged.)

To quantify the damage, we used a simple damage index (I_D) based on the Euclidian norm between a spectrum and a baseline spectrum. The root mean square deviation (RMSD) formula used was:

$$I_D = \sqrt{\frac{\sum_N [\text{Re}(Z_i) - \text{Re}(Z_i^0)]^2}{\sum_N [\text{Re}(Z_i^0)]^2}}, \quad (4)$$

where N is the number of points considered in the spectrum, and the superscript 0 signifies the baseline spectrum. In our work, we considered the spectrum measured on the pristine specimen before any cracks were induced to be the baseline spectrum. Figure 4 shows the damage index plots. For PWAS #1, the damage index increases rapidly at first, as crack #0 approaches the PWAS and then crack #1 crosses the PWAS location. After the crack has passed the PWAS location, the damage index curve leveled off.

A similar situation is observed for the PWAS #2 and #3. Every time, large changes in the E/M impedance spectrum are observed as the crack tip approaches the PWAS location. Once the crack tip has passed the PWAS location, further changes are only marginal. For PWAS #2, these significant changes occur at cracks #3 and #4, when pronounced increases in peak amplitudes appear at around 200 kHz and 390 kHz, simultaneous with a downward shift of the peaks (see Fig. 3, PWAS #2 spectrum). The corresponding damage index for PWAS #2 also shows significant changes only when the crack tip crosses the PWAS location (Fig. 4(b)). Similar observations are also made for PWAS #3, only that in this case the changes occur around the last two cracks, #5 and #6 (Fig. 4(c)).

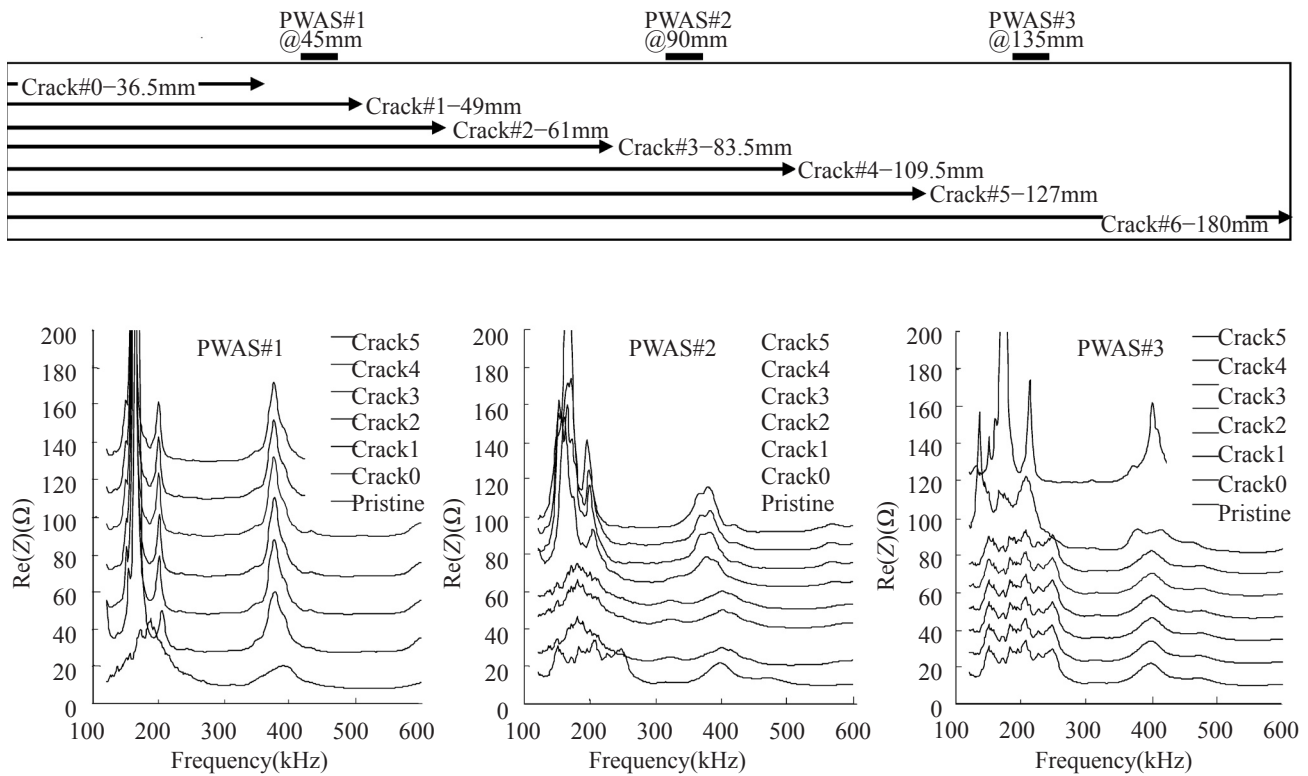


Fig. 3 High-frequency E/M impedance spectra for PWAS #1 through #3 on the coupon specimen: Note that as the crack advances towards each PWAS, the E/M impedance spectrum modifies significantly (vertical shifts have been applied during plotting to allow easy examination of the spectrum shape)

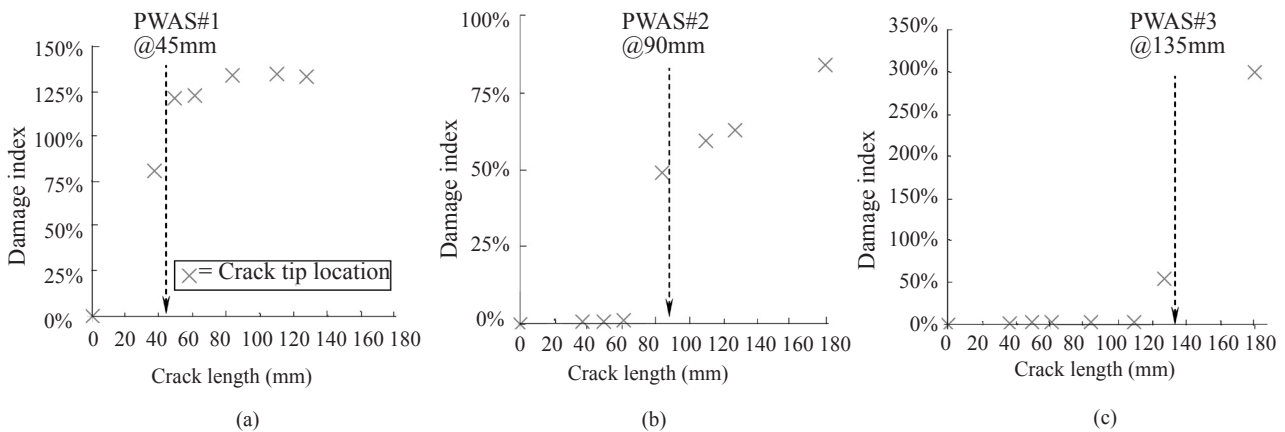


Fig. 4 Progression of damage index with crack length and damage location for PWAS #1 through #3. Note the dramatic change in damage index as the crack tip crosses below the PWAS location.

These coupon tests have demonstrated that the PWAS are able to detect the disbond crack presence in their vicinity, and are insensitive to cracks in the far field. Thus, they have both crack detection and crack locating capabilities when appropriately distributed. When the cracks are far away from the PWAS, the E/M impedance spectra are practically unchanged. But when the crack is close to the PWAS location, the detection is very strong. This detection localization property is possible only when using high-frequency vibration modes because the high-frequency vibration modes are highly localized and

hence sensitive to local damage, but rather insensitive to far-field damage. A damage metric expression based on the Euclidian norm and expressed as the root mean square deviation (RMSD) between a baseline spectrum and the currently measured spectrum was successfully used to quantify the disbond damage intensity.

3 Large scale tests

The large scale tests were used to verify the disbond detection capabilities of PWAS on realistic

civil engineering structures. A series of tests have been conducted at the University of South Carolina to assess the strength and durability of FRP composite overlay repairs, retrofit, and rehabilitation of civil engineering structures. Part of this wide effort includes exploring sensors and methods for detecting disbonds between the FRP composite overlay and the structural concrete substrate. In particular, the examination of the use of PWAS in conjunction with the E/M impedance technique to detecting disbonding was examined. Representative test results obtained during a fatigue test performed on an RC beam retrofitted with carbon fiber reinforced polymer are presented.

3.1 Reinforced concrete beam specimens

The fatigue test specimens used to demonstrate the PWAS disbond detection technique were taken from a series of specimens being tested to investigate a variety of CFRP composite retrofit techniques (Quattlebaum, 2003; Quattlebaum *et al.*, 2004). (In these cited studies, this test specimen was designated C-H). The test specimen (Fig. 5) consisted of a reinforced-concrete (RC) beam with adhesively bonded preformed CFRP strips applied to its soffit. The beam is 254 mm deep, 152 mm wide and was tested over a simple span of 4572 mm. The beam had three #4 (12.7 mm dia.) longitudinal internal steel reinforcing bars. The beam was designed such that it required no internal shear reinforcement. Concrete compressive strength was determined to be 29.5 MPa and the yield and tensile strength of the internal reinforcing steel was 446 MPa and 735 MPa, respectively. The beam was retrofitted with a 51 mm wide by 1.4 mm thick unidirectional preformed CFRP strip (Fyfe, 2004). The manufacturer's reported rupture strength and tensile modulus of the 1.4 mm thick CFRP strip are 3.9 kN/mm (width) and 216 kN/mm (width), respectively. The CFRP was bonded to the soffit of the concrete beams using a two part epoxy specified for the purpose and supplied by the CFRP supplier. The epoxy has a manufacturer's reported tensile strength and modulus of 72.4 MPa and 3.2 GPa, respectively. The CFRP was applied over the entire length of the beam although did not extend over the supports.

3.2 Test set up and protocol

Fatigue testing was performed at high stress range to achieve failure within a reasonable testing time. A concentrated load was applied to the beam midspan through a servo-controlled, fatigue-rated 490 kN capacity hydraulic actuator as shown in Fig. 5(b). The beam was instrumented for the measurement of deflection and strain. The deflection was measured at midspan of the beam. Longitudinal strains were measured on the reinforcing steel, on the beam exterior at the level of the reinforcing steel, and on the CFRP strip. The fatigue load regime consisted of cycling the midspan load between 7.5 kN and 28.9 kN at a frequency of

1.3 Hz. Strain readings on the internal reinforcing steel of specimen during the first fatigue cycle indicated reinforcing bar strains cycling from approximately 535 to 1590 microstrain or approximately 24% to 71% of the yield strain — a stress range of $0.47f_y$ or 211 MPa. Full sets of readings were taken during the loading cycles $N=1; 100; 1,000; 2,000; 5,000; 10,000; 20,000; 50,000; 100,000$; and at increments of 100,000 cycles thereafter.

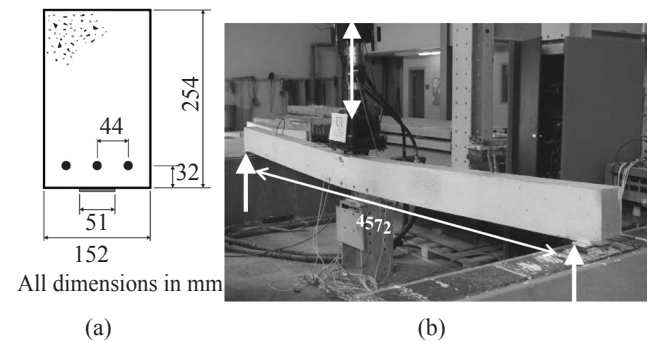


Fig. 5 Reinforced concrete beam specimen setup: (a) beam details; (b) test setup

3.3 Experimental results and observations

Figure 6 shows the applied load versus midspan deflection curves. The beam experienced a reinforcing bar rupture between 523 and 600 kilocycles. The CFRP remained intact and cycling was continued until a second reinforcing bar rupture occurred at 807,415 cycles. Post processing of strain data (Fig. 7) indicated that the strain in the CFRP composite overlay increased sharply after the rupture of the steel reinforcing bar. This increase is associated with redistribution of the load between the ruptured reinforcing steel and the composite overlay.

During the fatigue test, disbonding of the CFRP from the beam soffit was observed to occur. Exact measurements of the extent of disbonding are virtually impossible to obtain for this type of specimen. During the test, visual inspection was relied upon to identify disbonding, as hinted by changes observed in the sensor readings. The CFRP disbonding was initiated near the beam midspan (Fig. 8) and grew asymmetrically toward one beam support as fatigue loading continued. The asymmetry was biased towards the left end of the beam. (A companion specimen, loaded monotonically to failure exhibited similar disbonding behavior prior to eventual static failure of the beam, as reported by Quattlebaum (2003) and Quattlebaum *et al.* (2004). The initiation of disbonding was related to the internal steel reinforcement rupture that occurred between 523 and 600 kilocycles. Visually, the first disbonds were noticed as ~25mm delaminations in the vicinity of PWAS #30 at 600 kilocycles and in the vicinity of PWAS #28 at 700 kilocycles. As shown in Fig. 8, these disbonds were adjacent to vertical cracks in the concrete beam. As the fatigue cycles increased beyond 600 kilocycles towards the final failure at 807,415 cycles, the disbonds grew. When the rupture of the second reinforcing bar occurred

at 807,415 cycles, the existing disbonds grew to such an extent that the CFRP composite overlay completely detached itself to the left end of the beam, and remained attached only on the right hand side of the beam, from its right end termination to approximately one half of the distance along the span.

3.4 PWAS installation and monitoring

Eighteen PWAS were applied to the CFRP composite overlay after the composite overlay was attached the RC beam soffit. The work was performed with the beam in an inverted position. The PWAS were 2 mm diameter, 0.2 mm thick and weigh only 1 gram. The sensors were placed along the soffit a pitch of 15 mm, symmetrical about the beam centerline (Fig. 9(a)). The PWAS installation followed the procedure provided by Measurements Group, Inc. for the installation of electrical resistance strain gages. The CFRP was first

physically cleaned using a fine-edged mechanical scraper. Then, chemical cleaning was performed using M-LINE accessories degreaser, conditioner A, and neutralizer 5A. The PWAS were glued individually using the M-BOND 200 catalyst and adhesive system; pressure was applied with weights and protective padding until the adhesive was fully cured. The PWAS leads were wound and taped to the beam to protect them from damage during transportation to the testing apparatus. Once the girder was in place under the actuator and ready for testing, the lead wires were unraveled and their ends, positive and negative, were positioned on a platform for ease of organization and testing. Three meter lead wires were attached to the 52mm lead wires already present on each PWAS. The lead wires allowed measurement of the PWAS from a safe distance away from the specimen.

The E/M impedance of each PWAS was recorded with an HP4194A impedance analyzer. A custom LabView program interfaced with the HP4194A was

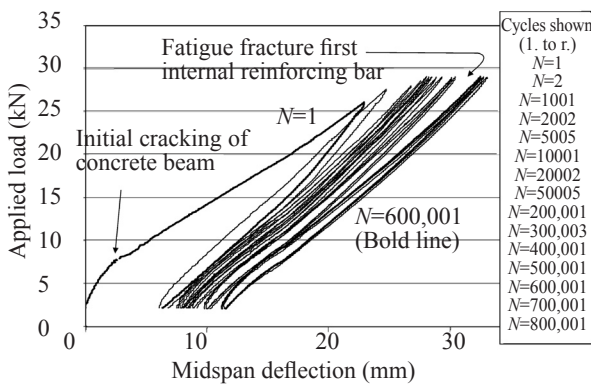


Fig. 6 Applied load versus midspan deflection for fatigue loaded specimen

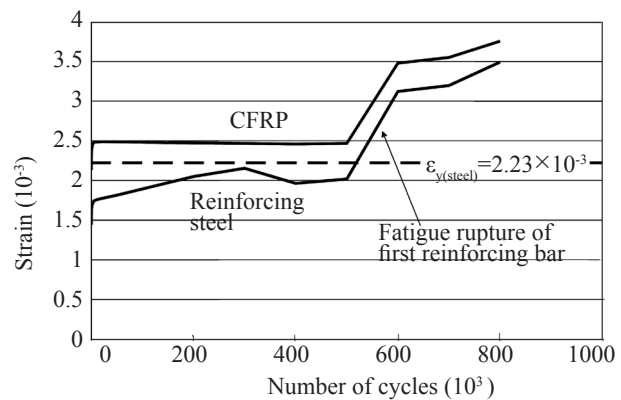


Fig. 7 Peak strains recorded during fatigue loading

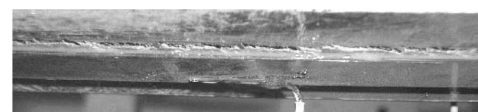
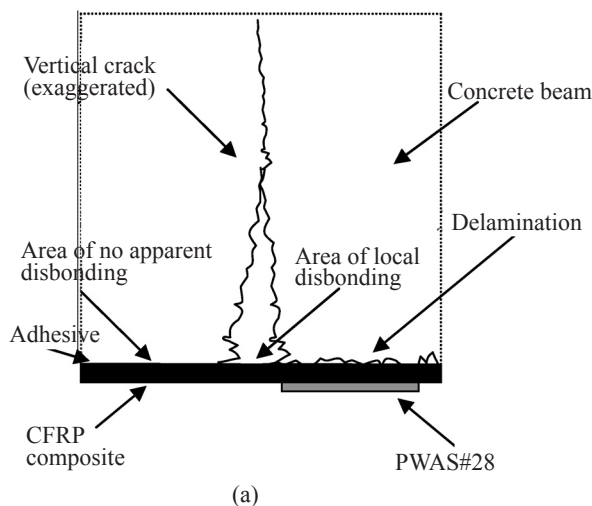


Fig. 8 Disbonding of the CFRP composite overlay observed visually during the test: (a) first small disbonds appeared after rupture of internal steel reinforcement between 523 and 600 kilocycles; (b) and (c): large disbonding observed at 800 kilocycles just prior to final failure

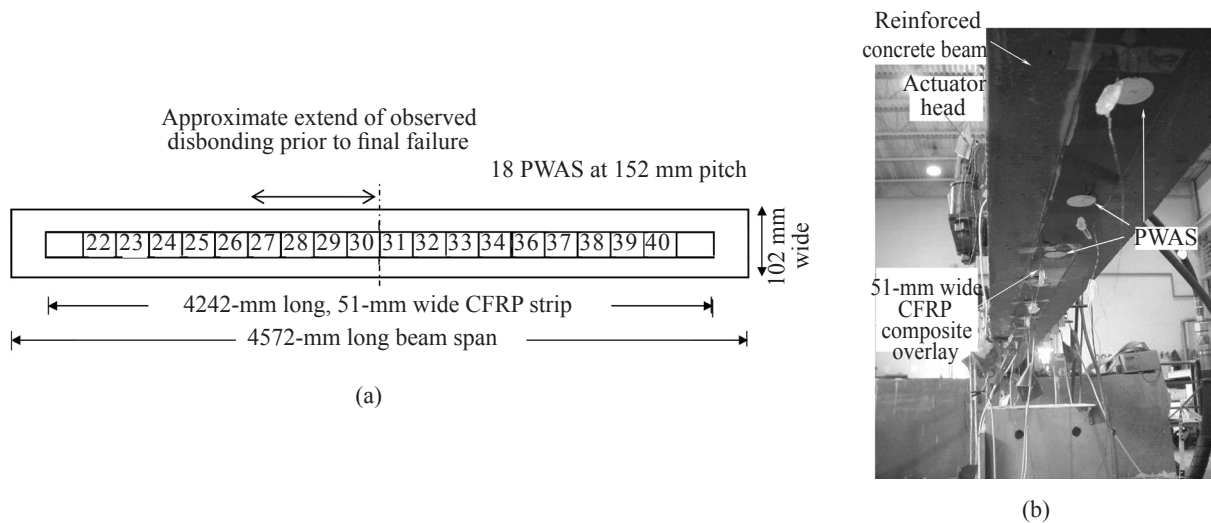


Fig. 9 Installation of PWAS disbond sensors for the large-scale tests of the RC beam reinforced with a CFRP composite overlay strip: (a) location and numbering (not to scale; PWAS #35 damaged during installation, replaced with PWAS #36); (b) photo of the experimental setup showing the installation and location of the PWAS disbond sensors.

used for data collection. Baseline readings were taken with all the instrumentation in place just before the start of the loading cycles, and after the first two loading cycles ($N = 1$ and 2). Because the first loading cycle resulted in initial (expected) cracking of the beam and some settling of the specimen on the test frame, the measurements from the second cycle ($N = 2$) were retained as the baseline for future comparison.

During the fatigue test, E/M impedance readings were taken at 300, 500, 600, 700, 800 kilocycles and after the 807 kilocycles final failure. After each reading was completed, the data from each PWAS was processed and analyzed to determine if any change or shift had occurred between the previous test and the present one. If a change was detected, the specimen was inspected visually for cracking or delamination, which might correspond to the change detected by the PWAS. The purpose of the visual inspection was to develop a method of predicting, through analysis of the PWAS data, the location, direction, and rate of disbonding between the CFRP overlay and the beam substrate.

3.5 E/M impedance spectroscopy for the large-scale tests

After the fatigue test was finished, the E/M impedance data was extensively post-processed. Superposition charts of the E/M impedance spectra evolution at each sensor were produced for each PWAS. Figure 10 presents two typical situations. The first situation (Fig. 10(a)) is that of PWAS #28, which was located below the disbond crack. The second situation (Fig. 10(b)) is that of PWAS #33, which was not located near the disbond crack (for exact PWAS locations see Fig. 9). As seen in Fig. 10(a), the PWAS #28 located above the disbond crack experienced a clear change in

the E/M impedance spectrum indicative of the presence of a disbond between the FRP composite overlay and the RC beam. To the naked eye, this spectral change seems to first appear at the 600 kilocycles reading and to progress onwards. This spectral change consists of the appearance and progression of a new spectral feature at around 350 kHz. Eventually, when the disbond was fully developed subsequent to beam failure, this feature grew into a distinct peak. The associated damage index calculated using Eq. (4) is presented in Fig. 11(a). The damage index curve presents three distinct sections. Below 500 kilocycles, little happens, indicative of insignificant disbond activity. However, the damage index at 500 kilocycles is slightly higher than that at lower kilocycles indicating some degradation. Between 500 and 800 kilocycles, a gradual progression of the damage index occurs; this can be directly correlated to the progression of the disbond crack between the composite overlay and RC beam substrate. From 800 kilocycles to the final failure at 807 kilocycles, the damage index increases dramatically, indicating a complete disbond situation with no residual contact to the concrete substrate.

In contrast, one can consider the situation of the PWAS #33 that was placed in a region that experienced no disbonds. Figure 10(b) indicates that no new spectral features appeared in the E/M impedance spectrum of this PWAS. Accordingly, the associated damage index (Fig. 11(b)) does not show any noticeable changes either. This situation is representative of the readings recorded on the PWAS that were placed away from disbond cracks. It indicates that the PWAS readings were not significantly affected by the large loads and the extensive load cycling applied during the fatigue test. This indirectly proves the durability and the survivability of the PWAS disbond sensors.

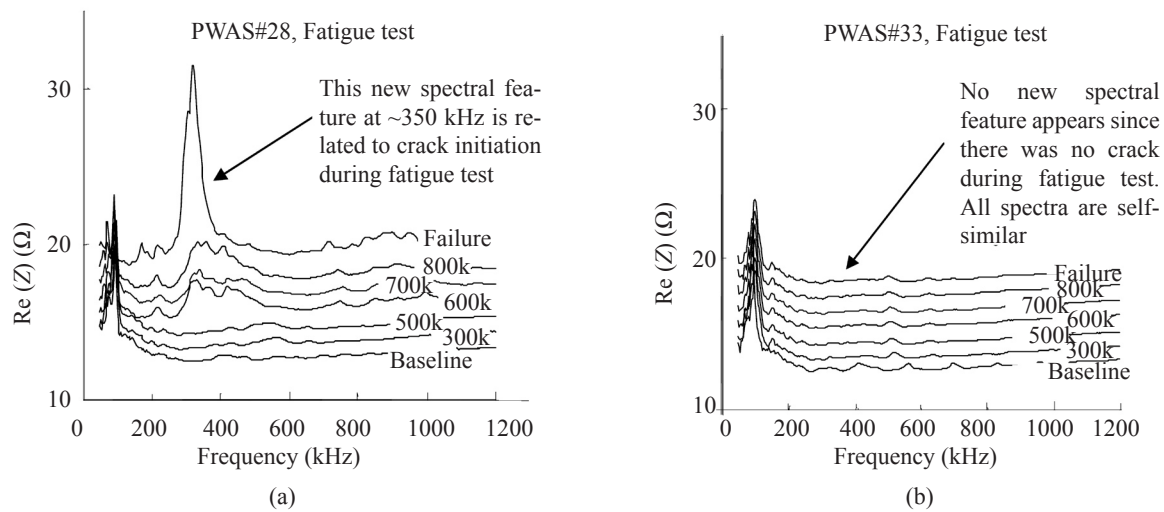


Fig. 10 Experimental verification of the E/M impedance method detection of disbonds during fatigue tests on concrete beams with surface-mounted FRP composite reinforcing strips: (a) PWAS #28 near a disbond crack shows a new spectrum feature related to crack initiation and propagation; (b) PWAS #33 away from any disbond cracks does not show any change in spectral pattern. Note: for clarity, curves are shifted upwards by fixed amounts.

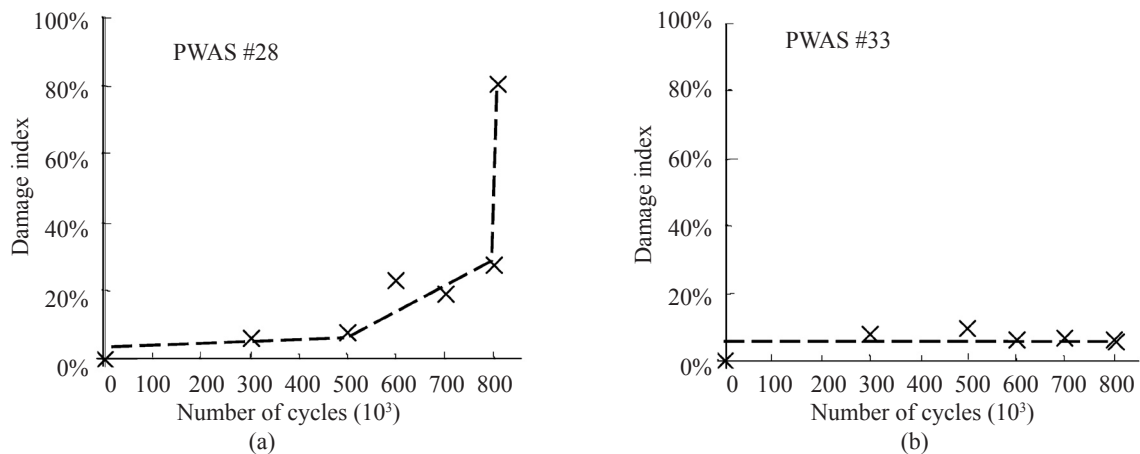


Fig. 11 Progression of damage index with number of kilocycles during RC beam fatigue: (a) PWAS #28 senses the presence and progression of the disbond crack through linear increase of damage index between 500 and 800 kilocycle. The steep ascent between 800 kilocycles and failure corresponds to the complete wide-area disbonding of the composite overlay; (b) in contrast, PWAS #33 (which was in a beam region with no disbond crack) does not show any significant damage index change

4 Summary and conclusions

This paper has presented a systematic investigation of the capabilities of piezoelectric wafer active sensors (PWAS) to detect disbonds between a fiber reinforced polymer (FRP) composite overlay and a concrete substrate using the electromechanical (E/M) impedance technique. The investigation was conducted in two stages: first, coupon tests were performed to develop the disbond detection methodology based on the changes in the E/M impedance spectrum in correlation with disbond cracks of various sizes. These coupon tests demonstrated that the PWAS are able to detect the presence of FRP disbonding in their vicinity, and are insensitive to damage in the far field. Thus, they have both crack detection and crack locating capabilities. When the cracks are far away from the PWAS, the

E/M impedance spectra are practically unchanged. But when the crack is close to the PWAS location, the detection is very strong. This detection locating property is possible only when using high-frequency vibration modes because the high-frequency vibration modes are highly localized and hence sensitive to local damage, but rather insensitive to far-field damage. A damage metric expression based on the Euclidian norm and expressed as the root mean square deviation (RMSD) between a baseline spectrum and the currently measured spectrum was successfully used to quantify the disbond damage intensity.

Large scale tests were used to verify the detection capabilities of PWAS on realistic civil engineering structures. A series of tests have been conducted at the University of South Carolina to assess the strength and durability of FRP composite overlay repairs, retrofit, and

rehabilitation of civil engineering structures. Part of this wide effort includes exploring sensors and methods for detecting disbonds between the FRP composite overlay and the structural concrete substrate. In particular the examination of the use of PWAS in conjunction with the E/M impedance technique to detecting disbonding was examined. Representative test results obtained during a fatigue test performed on an RC beam retrofitted with carbon fiber reinforced polymer are presented.

The large scale tests proved that the PWAS can successfully detect the presence and evolution of disbond cracks that appear between the FRP composite overlay and the RC beam substrate during fatigue testing. The damage locating property of these sensors has also been verified. Good correlation between the PWAS generated damage index and the physical progression of the fatigue crack was established. In addition, it was verified that the PWAS, when applied in accordance with the methodology described in this paper, can withstand large loads and extended cycling without degradation of their sensing properties (through 807,000 cycles as demonstrated in this experiment). The technique seems also able to predict incipient damage at an early stage before being reliably observable under visual inspection.

To the authors' knowledge, this is the first time that this particular health monitoring technique has been applied to the detection of disbonds between an FRP composite overlay and a RC structure during a large-scale fatigue test. The advantages of the PWAS technology for remotely monitoring disbond initiation and progression are apparent. However, further work is needed to establish the full understanding of this novel crack detection technique, to map its full capabilities and possible limitations, and to ascertain its advantages and disadvantages in comparison with other disbond crack detection methods.

Acknowledgements

Partial support from the National Science Foundation through grants NSF #CMS-9908293 and NSF INT-9904493, are thankfully acknowledged. The large-scale beams were tested as part of a study funded by the Federal Highway Administration and the South Carolina Department of Transportation (Project Number 614).

References

- ACI (1987), *Considerations for Design of Concrete Structures Subjected to Fatigue Loading*, American Concrete Institute.
- Ayres T, Chaudhry Z and Rogers C (1996), "Quality Health Monitoring of Steel Bridge Joint via Piezoelectric Actuator/Sensor Patches," *Proceedings, SPIE's 1996 Symposium on Smart Structures and Integrated Systems, SPIE*, **2719**: 123-131.
- Bhalla S and Soh CK (2003), "Structural Impedance Based Damage Diagnosis by Piezo-transducers," *Earthquake Engineering and Structural Dynamics*, **32**(12): 1897-1916.
- Bois C and Hochard C (2002), "Measurement and Modeling for the Monitoring of Damaged Laminate Composite Structures," *1st European Workshop on Structural Health Monitoring*, July 10-12, 2002, Paris, France, pp. 425-432.
- Buyukozturk O and Hearing B (1998), "Failure Behavior of Precracked Concrete Beams Retrofitted with FRP," *ASCE Journal of Composites for Construction*, **2**(3): 138-144.
- Cudney HH and Inman DJ (1998), "Piezoelectric Impedance-Based Qualitative Health Monitoring," *4th ESSM and 2nd MIMR Conference*, G. R. Tomlinson and W. A. Bulloch (Editors), Harrogate, U.K., pp. 795-785.
- Fyfe Company LLC (2000), *Tyfo UC Composite Laminate Strip System*, Material Specification Sheet.
- Giurgiutiu V, Reynolds A and Rogers CA (1999), "Experimental Investigation of E/M Impedance Health Monitoring of Spot-Welded Structural Joints," *Journal of Intelligent Material Systems and Structures*, Technomic Pub., USA, **10**(10): 802-812.
- Giurgiutiu V and Rogers CA (1999), "Recent Progress in the Application of E/M Impedance Method to Structural Health Monitoring, Damage Detection and Failure Prevention," *2nd International Workshop of Structural Health Monitoring*, Sept. 8-10, 1999, Stanford U., CA, pp. 298-307.
- Giurgiutiu V and Zagrai AN (2001), "Embedded Self-Sensing Piezoelectric Active Sensors for Online Structural Identification," *ASME Journal of Vibration and Acoustics*, **124**: 116-125.
- Giurgiutiu V, Lyons J, Petrou M., Laub D and Whitley S (2001), "Fracture Mechanics Testing of the Bond between Composite Overlays and Concrete Substrate," *Journal of Adhesive Science and Technology*, VSP International Science Pub., The Netherlands, **15**(11): 1351-1371.
- Giurgiutiu V, Zagrai AN and Bao J (2002), "Piezoelectric Wafer Embedded Active Sensors for Aging Aircraft Structural Health Monitoring," *Structural Health Monitoring – An International Journal*, **1**(1): 41-61.
- Koh YL and Chiu WK (2003), "Numerical Study of Detection of Disbond Growth Under a Composite Repair Patch," *Smart Materials and Structures*, **12**(4): 633-641.
- Liang C, Sun FP and Rogers CA (1994), "Coupled Electro-Mechanical Analysis of Adaptive Material System-Determination of the Actuator Power Consumption and System energy Transfer," *Journal of Intelligent Material Systems and Structures*, **5**: 12-20.
- Mallick PK (1993), *Fiber Reinforced Composites – Materials, Manufacturing, and Design*, Marcel Dekker, New York.

- Park G, Cudney H and Inman DJ (2000), "An Integrated Health Monitoring Technique using Structural Impedance Sensors," *Journal of Intelligent Material Systems and Structures*, **11**(6): 448-455.
- Pohl J, Herold S, Mook G and Michel F (2001), "Damage Detection in Smart CFRP Composites Using Impedance Spectroscopy," *Smart Materials and Structures*, **10**: 834-842.
- Quattlebaum JB (2003), "Comparison of Three CFRP Flexural Retrofit Systems under Monotonic and Fatigue Loads". *M.S. thesis*. Department of Civil and Environmental Engineering, University of South Carolina. 190 pp.
- Quattlebaum JB, Harries KA and Petrou MF (2004), "Static and Fatigue Behavior of Three CFRP Flexural Retrofit Systems," submitted to *ASCE Journal of Composites in Construction* (in review).
- Saffi MI and Sayyah T (2001), "Health Monitoring of Concrete Structures Strengthened with Advanced Composite Materials using Smart Piezoelectric Material," *Smart Materials and Structures*, **11**: 317-329.
- Sebastian MW (2001), "Significance of Midspan Debonding Failure in FRP-Plated Concrete Beams," *ASCE Journal of Structural Engineering*, **127**(7): 792-798.
- Shah SP, Swartz SE and Ouyang C (1995), *Fracture Mechanics of Concrete*, John Wiley & Sons.
- Soh CK, Tseng KK-H, Bhalla S and Gupta A (2000), "Performance of Smart Piezoelectric Patches in Health Monitoring of RC Bridge," *Smart Materials and Structures*, **9**(4): 533-542.
- Sun FP, Liang C and Rogers CA (1994), "Experimental Modal Testing Using Piezoceramic Patches as Collocated Sensors-Actuators," *Proceeding of the 1994 SEM Spring Conference & Exhibits*, Baltimore, MI, June 6-8, 1994.
- Triantafillou TC and Matthys S (2001), "Flexural Strengthening with Externally Bonded FRP Reinforcement," *Composites in Construction: A Reality, Proceedings of the International Workshop*, July 20-21, 2001, Capri, Italy, 194-202.
- Tseng KK, Tinker ML, Lassiter JO and Peairs DM (2003), "Temperature Dependency of Impedance-based Nondestructive Testing," *Experimental Techniques*, **27**(5): 33-36.
- Tseng KT, Basu PK and Wang L (2002), "Damage Identification of Civil Infrastructures Using Smart Piezoceramic Sensors," *1st European Workshop on Structural Health Monitoring*, July 10-12, 2002, Paris, France, pp. 450-457.
- Williams, J. G. (1984), *Fracture Mechanics of Polymers*, Ellis Harwood Ltd.
- Zagrai A and Giurgiutiu V (2001), "Electro-Mechanical Impedance Method for Crack Detection in Thin Plates," *Journal of Intelligent Material Systems and Structures*, **12**(10): 709-718.